

UDC 548.73:543.422:546.75:546.21

SPECTROSCOPIC CHARACTERIZATION AND ROOM-TEMPERATURE
STRUCTURE OF BIS(4-AMINOPYRIDINIUM) DICHROMATER. Ben Smail^{1,3}, H. Chebbi^{2,3}, B.R. Srinivasan⁴, M.F. Zid³¹University of Carthage, Nabeul Preparatory Engineering Institute, University Campus, Nabeul, Tunisia²University of Tunis, Tunis Preparatory Engineering Institute, Montfleury, Tunis, Tunisia

E-mail: chebhamouda@yahoo.fr

³University of Tunis El Manar, Faculty of Sciences of Tunis, Department of Chemistry, Laboratory of Materials, Crystallochemistry and Applied Thermodynamics, Farhat Hached University Campus, Tunis, Tunisia⁴Department of Chemistry, Goa University, Goa, India

Received June, 23, 2015

Revised — August, 10, 2015

Crystals of bis(4-aminopyridinium) dichromate ($C_5H_7N_2$)₂[Cr₂O₇] (**1**) were isolated via slow solvent evaporation and characterized by energy dispersive spectroscopy (EDS), infrared (IR) and ultraviolet-visible (UV-Vis) spectroscopy, and single crystal X-ray diffraction. The room-temperature (RT; 298 K) phase of **1** crystallizes in the monoclinic space group $P2_1/m$. Its asymmetric unit consists of two crystallographically independent 4-aminopyridinium cations (A and B) and two halves of symmetry-independent dichromate anions (A and B). Cations and anions are linked with the aid of several moderate N—H···O hydrogen bonds and weak C—H···O interactions resulting in a three-dimensional supramolecular network. The crystal structure is further stabilized by extensive π — π stacking interactions between adjacent pyridine rings. A comparison of the structure of the RT phase of **1** and that of the low temperature (LT; 150 K) phase is described.

DOI: 10.15372/JSC20170412

Keywords: crystal structure, infrared spectroscopy, bis(4-aminopyridinium) dichromate.

INTRODUCTION

Dichromates are an important class of compounds, which are extensively used in organic synthesis to effect a variety of synthetic transformations [1—3]. In a pioneering study, Corey and Schmidt [4] introduced bis(pyridinium) dichromate, known as PDC to organic chemists, as a mild reagent for the oxidation of alcohols. This work resulted in the development of several new oxidising agents like polyvinylpyridinium dichromate (PVPDC) [5], bis(benzyltriethylammonium) dichromate (BTEADC) [6], nicotinium dichromate (NDC) [7], isonicotinium dichromate (INDC) [7], bis(quinolinium) dichromate (QDC) [8], tetramethylethylenediammonium dichromate (TMEDADC) [9], piperazinium dichromate (PPDC) [10], imidazolium dichromate (IDC) [11], cetyltrimethylammonium dichromate (CTADC) [12], benzimidazolium dichromate (BIDC) [13] and quinoxalinium dichromate (QxDC) [14] in the last three and half decades. These reports demonstrate the possibility of isolation and characterization of the dichromate ion with different cations. Only four of these dichromates, *viz.* PDC [15], BIDC [16], PPDC [17] and QDC [18] have been structurally characterized. Other dichromates of N-heterocycles [19—31] and alkylammonium dichromates [32—40] have been the subject of only structural investigations. From structural point of view the dichromate ion offers several inte-

resting possibilities *viz.* its conformational flexibility in different environments, possibility to prepare noncentrosymmetric materials by choosing appropriate counter cation [41].

As part of an ongoing research program, our group has been involved in the synthesis and structural characterization of new organic dichromates over several years, which can be used for oxidation of organic substrates. Our investigations have unravelled a rich structural chemistry of dichromate compounds synthesised under mild reaction conditions using slow solvent evaporation at room temperature: tri(*N,N,N',N'*-tetramethylethylenediammonium) bis(dichromate) oxalate tetrahydrate ($C_6H_{18}N_2)_3(C_2O_4)[Cr_2O_7]_2 \cdot 4H_2O$ [42], *N,N,N',N'*-tetramethylethylenediammonium dichromate monohydrate $((CH_3)_2NH(CH_2)_2NH(CH_3)_2)[Cr_2O_7] \cdot H_2O$ [43], bis(ethylenediammonium) dichromate oxalate $(C_2H_{10}N_2)_2[Cr_2O_7](C_2O_4)$ [44], 1-cyclohexylpiperazine-1,4-dium dichromate $(C_{10}H_{22}N_2)Cr_2O_7$ [45], bis(guaninium) dichromate dihydrate $(C_5H_6N_5O)_2[Cr_2O_7] \cdot 2H_2O$ (Crystallographic data for the structure have been deposited with the Cambridge Crystallographic Data Centre, CCDC no. 1010792) and bis(1,3-bis(4-piperidinium)propane) dichromate trichromate monohydrate, $(C_{13}H_{28}N_2)_2[Cr_2O_7][Cr_3O_{10}] \cdot H_2O$ (CCDC no. 1043331). These materials were prepared by the reaction of chromium (VI) oxide with organic bases in water at ambient temperature and their structures were characterized by single crystal X-ray diffraction. In all these complexes the cations and the anions are linked by several hydrogen bonding interactions. A low temperature (LT) crystal structure of bis(4-aminopyridinium) dichromate has recently appeared in the literature [31]. In this paper we describe the synthesis, spectroscopic and structural characterization of the room-temperature (RT) phase of bis(4-aminopyridinium) dichromate, $(C_5H_7N_2)_2[Cr_2O_7]$ (**1**), and a comparison of the structures of the RT and LT phases.

EXPERIMENTAL

Synthesis of 1. To a solution of CrO_3 (1.77 g, 0.0177 mol) in distilled water (70 ml), 4-aminopyridine (0.65 g, 0.0069 mol) was added under stirring for 20 min in air. The reaction mixture solution was allowed to stand for a week at room temperature. Orange-red single crystals suitable for X-ray analysis were isolated on slow evaporation of the solvent.

EDS, IR and UV-visible analysis. A qualitative energy dispersive spectroscopy (EDS) analysis of some crystals was carried out using JEOL-JSM 5400 scanning electron microscope. Infrared (IR) measurement was performed at room temperature, on a Perkin-Elmer FT-IR Paragon 1000 PC spectrometer over the $4000\text{--}375\text{ cm}^{-1}$ region, by the KBr pellet method. Electronic spectrum was recorded on a Perkin-Elmer Lambda 19 spectrophotometer in the $200\text{--}900\text{ nm}$ range, using matched quartz cells, in H_2O as solvent.

Single crystal X-ray diffraction. A single crystal with dimensions $0.34 \times 0.24 \times 0.16\text{ mm}$ was chosen for the structure determination and refinement. It was selected under a polarizing microscope and was mounted on a Lindemann glass fiber. Intensity data were collected on an Enraf-Nonius four-circle diffractometer using graphite monochromated MoK_α radiation ($\lambda = 0.71073\text{ \AA}$). Lattice parameters and orientation matrix were obtained by the least-squares refinement of 25 reflections in the range $10.3\text{--}13.6^\circ$ using CAD4-EXPRESS program [46, 47].

The crystallographic data of **1**: $C_{10}H_{14}N_4O_7Cr_2$, $FW = 406.24$, $T = 298\text{ K}$, monoclinic, $P2_1/m$, $a = 7.714(2)$, $b = 16.351(3)$, $c = 12.397(2)\text{ \AA}$, $\beta = 94.57(3)^\circ$, $V = 1558.7(6)\text{ \AA}^3$, $Z = 4$, $\rho_{\text{calc}} = 1.731\text{ g/cm}^{-3}$, $\mu(MoK_\alpha) = 1.43\text{ mm}^{-1}$, a total of 3633 reflections ($\theta_{\text{min}/\text{max}} = 2.1^\circ/27^\circ$), 1860 observed reflections ($I \geq 2\sigma(I)$), 251 parameters. $GOOF = 1.00$, $R_1 = 0.047$, $wR_2 = 0.120$ ($I \geq 2\sigma(I)$), max/min diff. peak $0.42/-0.46\text{ e/\AA}^{-3}$.

The data reduction was processed with XCAD4 program [48] included in the WinGX software package [49]. The reflections were corrected for Lorentz and polarization effects; absorption correction was obtained via a psi-scan [50] and secondary extinction correction was applied too [50]. The structure was solved with direct methods using SHELXS-97 [51] and the refinement was done against F^2 using SHELXL-97 [51]. Anisotropic displacements were used for C, N, O and Cr atoms. Approximate positions for all the H atoms were first obtained from the difference electron density map. However, the H atoms were placed at their idealized positions and constrained to ride on their

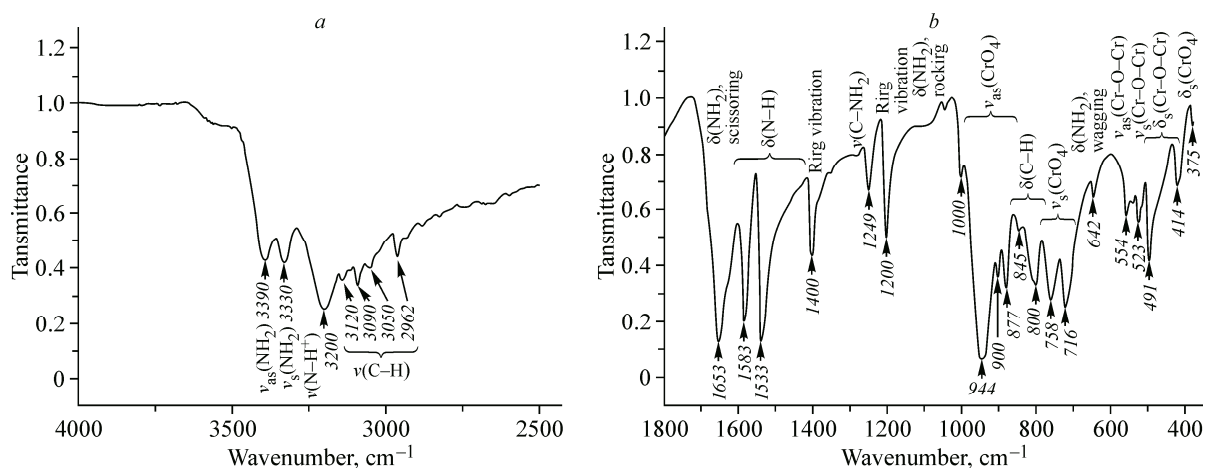


Fig. 1. IR spectrum of **1** at 298 K: 4000—2500 cm^{-1} range (a); 1800—375 cm^{-1} range (b)

parent atoms with isotropic temperature factors $U_{\text{iso}}(\text{H}) = 1.2U_{\text{eq}}(\text{N}, \text{C})$ and distances C—H = 0.95 and N—H = 0.88(1) Å using AFIX 43 and DFIX commands in SHELXL97, respectively. O4B oxygen of the dichromate anion B is disordered over two sites, viz. O4B and O4'B, with equal site occupancies of 0.5 for both. The structure graphics were drawn with Diamond Version 3.2e supplied by Crystal Impact [52]. CIF file containing complete information about the structure of **1** was deposited with the Cambridge Crystallographic Data Center (No. 1000545); the file is freely available upon request from the following web site: http://www.ccdc.cam.ac.uk/data_request/cif.

RESULTS AND DISCUSSION

EDS analysis. The EDS analysis of some crystals of **1** revealed the presence of Cr, O, and C elements, excluding hydrogen which is non-detectable with this method.

IR and UV-Vis spectroscopy. The infrared spectrum of **1** (Fig. 1) exhibits several signals in the mid-IR region indicating the presence of an organic moiety [53—56] and the dichromate group [20, 28, 57—62]. The bands observed in the infrared spectrum for the organic cation are consistent with the crystal structure reported here. The bands at 3390 and 3330 cm^{-1} belong to asymmetric and symmetric stretching vibrations of the —NH₂ groups of the primary amine, respectively. Absence of a wide band at 3020 cm^{-1} corresponding to NH₃⁺ group suggests that only the C=N groups of the aromatic ring were protonated. The band situated around 3200 cm^{-1} is assigned to the stretching vibration of the N—H⁺ in the aromatic ring involved in intermolecular hydrogen bonds. The stretching vibrations of C—H groups in the aromatic ring are observed around 3090 cm^{-1} . The peak at 1653 cm^{-1} is assigned to the scissoring (δ_{NH_2}) vibration. The bands at 1583 and 1533 cm^{-1} can be attributed to the N—H bending vibration. The bands at 1400 and 1200 cm^{-1} are due to pyridine skeleton vibrations. The bending vibrations of N—H and C—H groups appear in 850—780 cm^{-1} range. The peak at 1249 cm^{-1} corresponds to the C—NH₂ stretching vibration ($\nu_{\text{C-NH}_2}$).

Asymmetric and symmetric stretching vibrations of the Cr—O terminal bond are observed in 1000—860 and 780—670 cm^{-1} regions, respectively. The peaks around 554 and 523 cm^{-1} are assigned to the asymmetric and symmetric stretching modes of vibration of the Cr—O—Cr fragment. The bands in the 505—400 cm^{-1} range can be attributed to the Cr—O—Cr bending vibrations. Finally, the band around 375 cm^{-1} can be assigned to the symmetric bending mode of vibration of the Cr—O terminal bonds. The electronic spectrum of an aqueous solution of **1** exhibits bands at 352 and 262 nm characteristic of the dichromate chromophore [59, 63].

X-ray crystallography. The molecular structure of the room-temperature phase of **1** is shown in Fig. 2. The asymmetric unit is composed of two crystallographically independent 4-aminopyridinium cations (A and B) and two halves of symmetry-independent dichromate anions (A and B). The cations

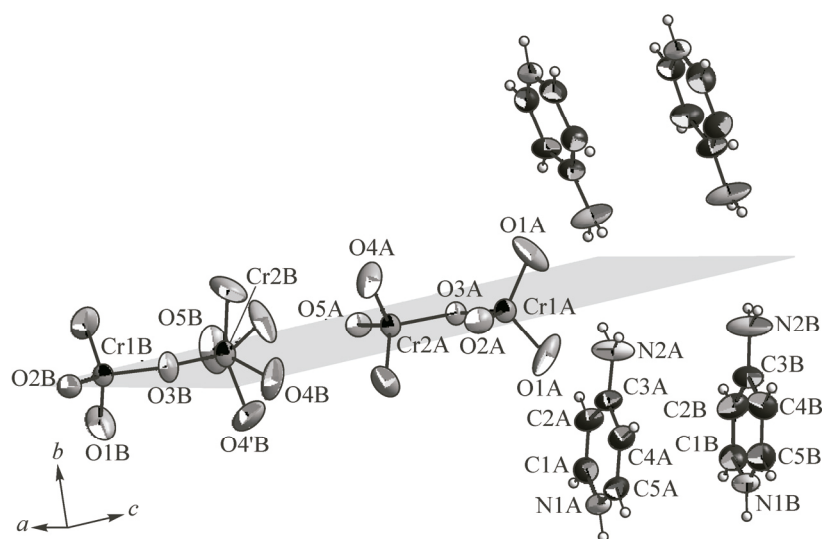


Fig. 2. The molecular structure of **1** at 298 K. Displacement ellipsoids are shown at the 50 % probability level. Only the symmetry independent non-hydrogen atoms are labelled

occupy general positions, whereas the anions are located on a mirror plane. The crystal structure displays intricate hydrogen bonding interactions between organic cations and inorganic anions.

The pyridine rings of organic cations A and B possess almost planar geometry with an r.m.s. deviation from the mean plane of 0.0041 Å and 0.0030 Å, respectively, and form a dihedral angle of 2.5(2)°. These cations are stacked approximately face-to-face to form columns along the $[-1\ 0\ 1]$ direction (Fig. 3). The centroid—centroid distances between adjacent pyridine rings A—A, B—B and A—B are 3.709(9), 3.80(1) and 3.91(1) Å, respectively. The shortest interplanar distance A—A is shorter than 3.80 Å, indicating π — π stacking interactions [64].

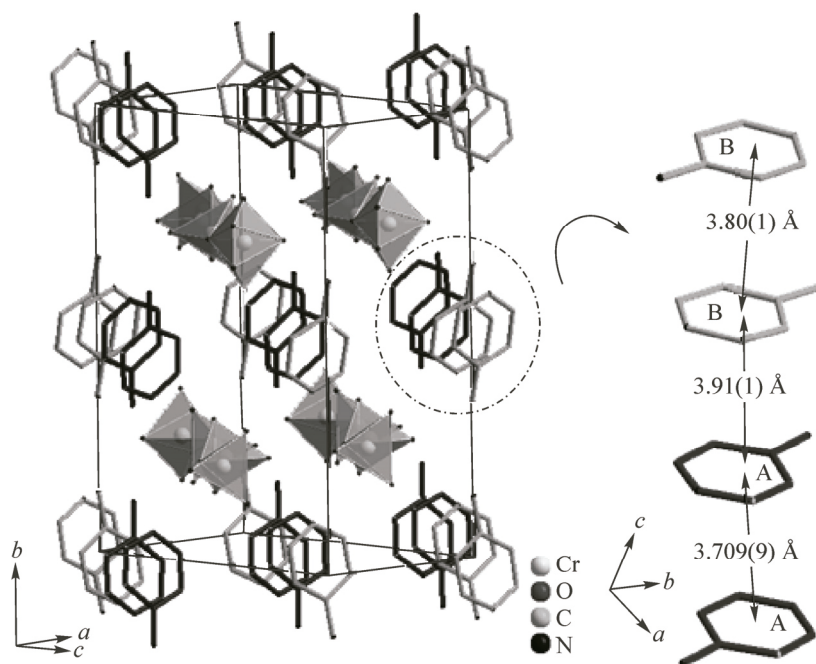


Fig. 3. Perspective view of the crystal structure of **1** at 298 K, showing the arrangement of 4-aminopyridinium into columns running along the $[-1\ 0\ 1]$ direction. The hydrogen atoms have been omitted for clarity

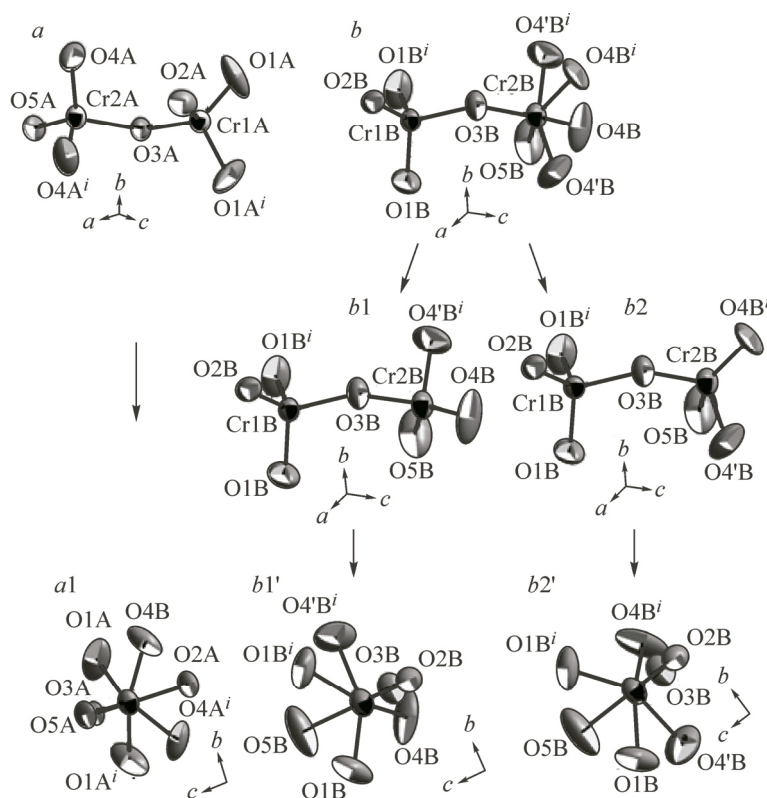


Fig. 4. Dichromate anions A and B in the structure of **1** at 298 K (a), (b); the two $\text{Cr}_2\text{O}_7^{2-}$ subunits present in dichromate anion B (b1), (b2). Projection of anion A along the Cr—Cr direction (a1). Projection of the two $\text{Cr}_2\text{O}_7^{2-}$ groups of anion B along the Cr—Cr direction (b1'), (b2').

Symmetry code: $\frac{1}{2}x, -y+3/2, z$

The nitrogen atom of the pyridine ring is protonated. The protonation of atoms N1A and N1B leads to a slight increase in the C5A—N1A—C1A ($121.7(4)^\circ$) and the C1B—N1B—C5B ($121.4(4)^\circ$) angles compared to those observed in the structure of free 4-aminopyridine [65, 66]. A decrease in the C3A—N2A ($1.316(6) \text{ \AA}$) and C3B—N2B ($1.330(6) \text{ \AA}$) bond lengths was also observed. Both nitrogen atoms of 4-aminopyridinium are involved in an extensive hydrogen bonding network. The bond lengths and angles for $\text{C}_5\text{H}_7\text{N}_2^+$ cations are typical of the protonated forms of 4-aminopyridine derivatives [55, 67—74].

The dichromate anions A and B are located on a mirror plane that passes through O2A, O3A, O5A and O2B, O3B, O5B respectively. The anion (B) exhibits disorder of the terminal O4 atom around the mirror plane over two positions O4B and O4'B in a ratio 1:1. Fig. 4 shows the two $\text{Cr}_2\text{O}_7^{2-}$ subunits present in dichromate anion B. This type of disorder has also been observed in the crystal structure of bis(dihexadecyldimethylammonium) dichromate [35], N,N,N',N'-tetramethylethylenediammonium dichromate monohydrate [42], bis(ethylenediammonium) dichromate oxalate [44], and $(\text{Hdpam})_2\text{Cr}_2\text{O}_7$ [20]. Contrary to the quasi-eclipsed conformation generally encountered in alkali dichromates [75, 76], this one exhibits a surprising staggered conformation: the tetrahedral twist about $50.787(14)$ to $72.906(19)^\circ$ (Fig. 4, a1, b1' and b2') away from the exactly eclipsed conformation in such a way that the three-fold symmetry axis disappears.

The Cr—O terminal bond lengths are in the range $1.518(7)$ — $1.712(7) \text{ \AA}$ and the bridging Cr—O bonds are longer and in the range $1.790(4)$ — $1.803(4) \text{ \AA}$. The anions A and B have a bent Cr—O—Cr bridging angle of $121.9(2)^\circ$ and $129.0(2)^\circ$, respectively. The various geometrical parameters observed

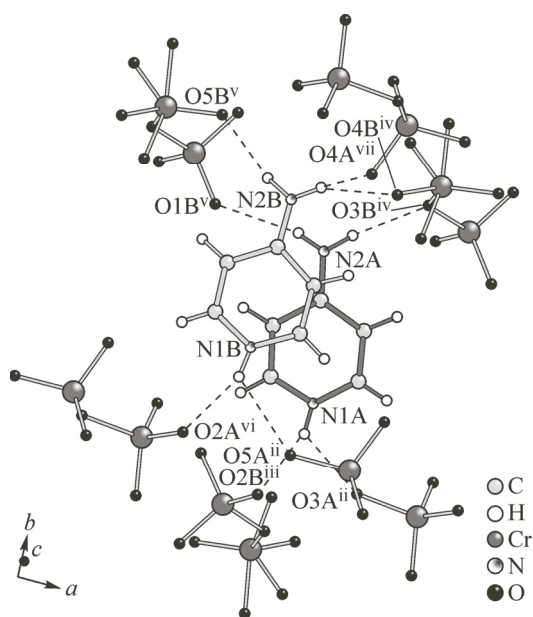


Fig. 5. Part of the crystal structure of **1** at 298 K, showing N—H...O hydrogen bonds.

Symmetry codes: ⁱⁱ $-x+1, y-1/2, -z+1$; ⁱⁱⁱ $-x+1, y-1/2, -z$; ^{iv} $x, y, z+1$; ^v $x-1, y, z+1$; ^{vi} $-x, y-1/2, -z+1$; ^{vii} $x, -y+3/2, z+1$

in the Cr_2O_7 moieties agree well with previously determined structures [16, 22, 24, 25, 32, 34–36, 38, 42–44].

The structure of **1** consists of alternating columns of discrete 4-aminopyridinium cations and of discrete dichromate anions extending along the crystallographic $[-1\ 0\ 1]$ direction. Every organic column, $\{\text{C}_5\text{H}_7\text{N}_2^+\}_n$, is surrounded by four inorganic columns, $\{\text{Cr}_2\text{O}_7^{2-}\}_n$, and vice versa (Fig. 3).

The dichromate anions and the 4-aminopyridinium cations are linked by N—H...O hydrogen bonds with N...O distances varying between 2.906(5) and 3.139(6) Å. The moderate H bonds [77] involve oxygen

atoms of the dichromate anions as acceptors, and the protonated nitrogen atoms of 4-aminopyridinium as donors (Fig. 5). There are also long C—H...O interactions with C...O bond lengths ranging from 3.204(6)—3.389(6) Å. These interactions between oxygen atoms of the anions and the carbon atoms of the cations cannot be considered to be hydrogen bonds, but they are indicative of some degree of polarization [20]. The role of this type of interaction in organic dichromates has been examined previously [18, 20–22, 24–26, 28, 39, 42]. The electrostatic interactions and H-bonds interlink columns to keep up the three-dimensional network cohesion. Furthermore, π — π interactions between adjacent pyridine rings help to stabilize the crystal packing, the closest distance between two pyridine mean planes being 3.709(9) Å (Fig. 3).

The structure of **1** collected at room temperature (RT; $T = 298\text{ K}$) is compared with that determined at low temperature (LT; $T = 150\text{ K}$) [31]. The LT structure has space group $P2_1/c$ and cell parameters $a = 13.8505(4)\text{ Å}$, $b = 16.2486(4)\text{ Å}$, $c = 15.2586(4)\text{ Å}$, $\beta = 118.923(2)^\circ$. The RT structure has space group $P2_1/m$, and cell parameters $a = 7.714(2)\text{ Å}$, $b = 16.351(3)\text{ Å}$, $c = 12.397(2)\text{ Å}$, $\beta = 94.57(3)^\circ$, but can be redescribed using new axes $\mathbf{a}' = -\mathbf{a} - \mathbf{c}$, $\mathbf{b}' = \mathbf{b}$, $\mathbf{c}' = \mathbf{a}$, to give the cell $a' = 14.070(4)\text{ Å}$, $b' = 16.351(3)\text{ Å}$, $c' = 7.714(2)\text{ Å}$, $\beta' = 118.56(2)^\circ$ and space group $P2_1/m$. The relationships as regards passage from LT phase to RT phase for the cell parameters are: $a'(\text{RT}) \cong a(\text{LT})$, $b'(\text{RT}) \cong b(\text{LT})$, $c'(\text{RT}) \cong c(\text{LT})/2$ (Fig. 6). A comparison of cell parameters and crystal structures of these two phases reveal that there is a transition from RT lattice to LT lattice by the doubling of its c axis length and the unit cell volume accompanied by the loss of the mirror which becomes a glide plane. In these condi-

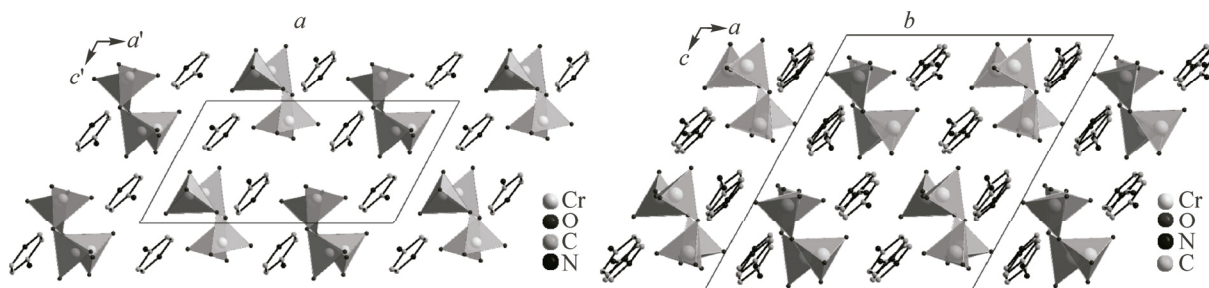


Fig. 6. Projection of the structure of **1** along the $[0\ 1\ 0]$ direction (a) the room temperature structure using the new axis $\mathbf{a}' = -\mathbf{a} - \mathbf{c}$, $\mathbf{b}' = \mathbf{b}$, $\mathbf{c}' = \mathbf{a}$ (b) the low temperature structure. The hydrogen atoms have been omitted for clarity

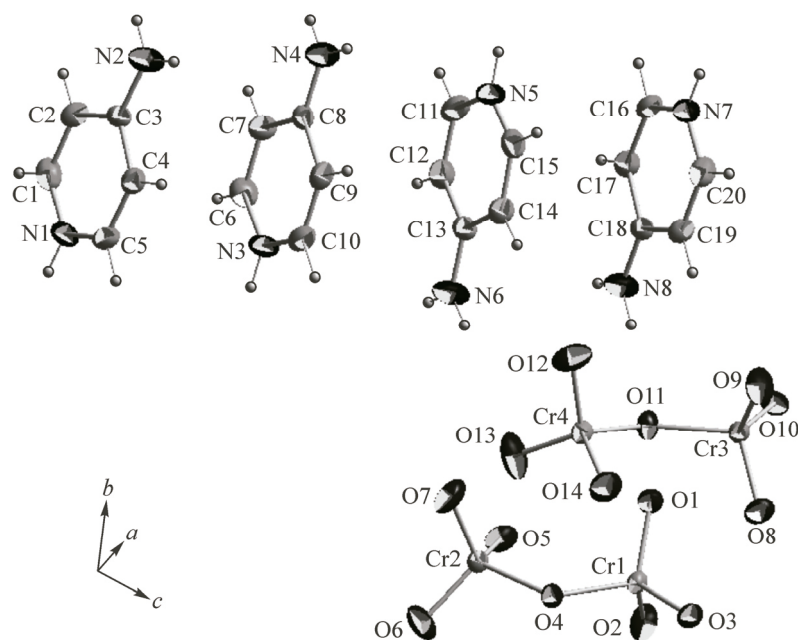


Fig. 7. The molecular structure of **1** at 150 K. Displacement ellipsoids are shown at the 50 % probability level. Only the oxygen and chromium atoms are labelled

tions, the space group, which was $P2_1/m$ with $Z = 4$ for the RT structure becomes $P2_1/c$ with $Z = 8$ in LT structure. In RT phase, the asymmetric unit consists of two crystallographically independent 4-aminopyridinium cations and two halves of symmetry independent dichromate anions whereas in the LT phase it is composed of four crystallographically independent 4-aminopyridinium cations and two independent dichromate anions (Figs. 2 and 7).

In the RT structure, the dichromate anion (B) exhibits disorder of O4B atom around the mirror over two positions in a 1:1 ratio but in LT structure, all oxygen atoms of dichromate anions were ordered. It is noteworthy that in the RT structure there is a mirror plane, lying on the atoms of the dichromate anion A (Cr1A, Cr2A, O2A, O3A and O5A) and atoms of the dichromate anion B (Cr1B, Cr2B, O2B, O3B and O5B), corresponding well to its mirror symmetry $m(x, 1/4, y)$. When the temperature decreases (in the LT phase), the disordered O4B atom of the dichromate anion (B) is eventually frozen into ordering. During this process, the mirror plane disappears, owing to reorientation of the dichromate anions. The loss of this plane can also be deduced from molecular configuration of dichromate anions. In RT the torsion angles of O5A—Cr2A—O3A—Cr1A, O2A—Cr1A—O3A—Cr2A, O5B—Cr2B—O3B—Cr1B and O2B—Cr1B—O3B—Cr2B were calculated to be 180, 0, 0 and 180° respectively which strongly support the presence of the symmetric plane. However, these values become $-176.8(1)$, $-13.4(1)$, $-34(1)$ and $-166(1)^\circ$ for O3—Cr1—O4—Cr2, O5—Cr2—O4—Cr1, O14—Cr4—O11—Cr3 and O10—Cr3—O11—Cr4, respectively, in the LT structure, revealing that the dichromate anions undergo small angle twisting motion. The packing in both RT and LT phases involves alternating columns of discrete 4-aminopyridinium cations and of discrete dichromate anions with staggered conformation (mentioned as eclipsed by Sonia Trabelsi and co-workers [31] which seems to be incorrect) extending along the crystallographic $[-1\ 0\ 1]$ direction for RT structure (Fig. 3) and $[1\ 0\ 1]$ direction for LT structure.

CONCLUSIONS

The synthesis, spectroscopic characterization and X-ray structure of the room-temperature phase of bis(4-aminopyridinium) dichromate are described. The reaction of CrO_3 with the aromatic amine in water followed by slow evaporation of the solvent is a convenient method to prepare the title com-

pound. The infrared spectrum of the complex is fully consistent with its crystal structure. The protonation of the pyridine nitrogen atom and not on the amino group is thus confirmed. The title compound crystallizes in a monoclinic centrosymmetric structure built up as a succession of organic columns formed of discrete 4-aminopyridinium cations alternated with inorganic columns made of discrete dichromate anions parallel to the $[-1\ 0\ 1]$ direction linked together by moderate hydrogen-bonding $N-H\cdots O$ and the weak intermolecular $C-H\cdots O$ interactions in a 3D network.

The comparison of cell parameters and crystal structure of the RT-phase of **1** to the LT-phase reveals that there is a transition from RT lattice to LT lattice by doubling the c axis length and the unit cell volume, accompanied by the loss of the mirror which becomes a glide plane.

The crystal data collection of **1** was done in the Laboratory of Materials, Crystallochemistry and Applied Thermodynamics, Department of Chemistry, Faculty of Sciences of Tunis, University of Tunis El Manar, Tunis, Tunisia. We are grateful to Professor Ahmed Driss who supervised this research.

The authors gratefully acknowledge the financial support of Ministry of Higher Education, Scientific Research and Technology of Tunisia.

REFERENCES

1. House H.O. Modern Synthetic Reactions, 2nd edn. W.A. Benjamin Inc., Menlo Park, California, 1972.
2. Furniss B.S., Hannaford A.J., Rogers V., Smith P.W.G., Tatchell A.R. Vogel's Textbook of Practical Organic Chemistry, 5th edn. ELBS, London, 1989.
3. Carruthers W., Coldham I. Modern methods of organic synthesis, 4th edn. – London: Cambridge University Press, 2004.
4. Corey E.J., Schmidt G. // Tetrahedron Lett. – 1979. – **20**. – P. 399 – 402.
5. Fréchet J.M.J., Darling P., Farrall M.J. // J. Org. Chem. – 1981. – **46**. – P. 1728 – 1730.
6. Miaorong T., Huang X., Chen Z., Hangzhou D.X. // Ziran Kexueban. – 1984. – **11**. – P. 454.
7. López C.M., González A., Cossío F.P., Palomo C. // Synthetic Commun. – 1985. – **15**. – P. 1197 – 1211.
8. Balasubramanian K., Prathiba V. // Indian. J. Chem. – 1986. – **25B**. – P. 326 – 327.
9. Chandrasekhar S., Takhi M., Mohapatra S. // Synthetic Commun. – 1996. – **26**. – P. 3947 – 3951.
10. Movassagh B., Lakouraj M.M., Ghodrati K. // Indian J. Chem. – 2002. – **B41**. – P. 1293 – 1295.
11. De S.K. // Synthetic Commun. – 2004. – **34**. – P. 2751 – 2755.
12. Patel S., Mishra B.K. // Tetrahedron Lett. – 2004. – **45**. – P. 1371 – 1372.
13. Meng Q.H., Feng J.C., Bian N.S., Liu B., Li C.C. // Synthetic Commun. – 1998. – **28**. – P. 1097 – 1102.
14. Değirmenbaşı N., Özgün B. // Monatshefte für chemie. – 2002. – **133**. – P. 1417 – 1421.
15. Lennartson A., Håkansson M. // Acta Cryst. – 2009. – **C65**. – P. m182 – m184.
16. Meng Q., Yan W., Xu S., Huang D. // J. Chem. Crystallogr. – 2004. – **24**. – P. 333 – 336.
17. Srinivasan B.R., Naik A.R., Näther C., Bensch W. // Acta Cryst. – 2004. – **E60**. – P. m1384 – m1386.
18. Sundar T.V., Parthasarathi V., Thamocharan S., Sekar K.G. // Acta Cryst. – 2003. – **E59**. – P. m327 – m329.
19. Cameron T.S., Clyburne J.A.C., Dubey P.K., Grossert J.S., Ramaiah K., Ramanatham J., Sereda S.V. // Can. J. Chem. – 2003. – **81**. – P. 612 – 619.
20. Martín-Zarza P., Gili P., Rodríguez-Romero F.V., Ruiz-Pérez C. // Polyhedron. – 1995. – **14**. – P. 2907 – 2917.
21. Jin Z.M., Zhang H.M., Wang H.B., Hu M.L., Shen L. // Acta Cryst. – 2004. – **C60**. – P. m572 – 574.
22. Jin Z.M., Ma X.J., Zhang Y., Tu B., Hu M.L. // Acta Cryst. – 2006. – **E62**. – P. m106 – m108.
23. Sieron L. // Acta Cryst. – 2007. – **E63**. – P. m2068.
24. Sieron L. // Acta Cryst. – 2007. – **E63**. – P. m2336.
25. Akriche S., Rzaigui M. // Acta Cryst. – 2009. – **E65**. – P. m123.
26. Pressprich M.R., Willett R.D., Sheets R.M., Paudler W.W., Gard G.L. // Acta Cryst. – 1990. – **C46**. – P. 1635 – 1637.
27. Gholizadeh M., Pourayoubi M., Kia M., Rheingold A.L., Golen J.A. // Acta Cryst. – 2012. – **E68**. – P. m305.
28. Phetmung H., Wateh M., Pakawatchai C. // Turk J. Chem. – 2012. – **36**. – P. 556 – 556.
29. Zhu R.Q. // Acta Cryst. – 2012. – **E68**. – P. m389.
30. Liu H.X. // Z. Kristallogr. – 2009. – **224**. – P. 717 – 718.
31. Trabelsi S., Roisnel T., Dhaouadi H., Marouani H. // Acta Cryst. – 2014. – **E70**. – P. m263 – m264.
32. Wajzman E., Cygler M., Grabowski M.J., Stepien A. // Roczn. Chem. – 1976. – **50**. – P. 1587 – 1592.
33. Lorenzo-Luis P.A., Martín-Zarza P., Gili P., Arrieta J.M., Germain G., Dupont L. // Acta Cryst. – 1995. – **C51**. – P. 1073 – 1075.
34. Fossé N., Caldes M., Joubert O., Ganne M., Brohan L. // J. Solid State Chem. – 1998. – **139**. – P. 310 – 320.

35. Fossé N., Brohan L. // J. Solid state Chem. – 1999. – **145**. – P. 655 – 667.
36. Fossé N., Joubert O., Ganne M., Brohan L. // Solid State Science. – 2001. – **3**. – P. 121 – 132.
37. Srinivasan B.R., Dhuri S.N., Nather C., Bensch W. // Indian J. Chem. – 2003. – **A42**. – P. 2735 – 2741.
38. Due-Hansen J., Ståhl K., Boghosian S., Riisager A., Fehrmann R. // Polyhedron. – 2011. – **30**. – P. 785 – 789.
39. Trabelsi S., Marouani H., Al-Deyab S.S., Rzaigui M. // Acta Cryst. – 2012. – **E68**. – P. m1056.
40. Jin L., Liu N.X. // Acta Cryst. – 2012. – **E67**. – P. m1586.
41. Pecaut J., Masse R. // Acta Cryst. – 1993. – **B49**. – P. 277 – 282.
42. Khadhrani H., Ben Smail R., Driss A. // C.R. Chimie. – 2006. – **9**. – P. 1322 – 1327.
43. Khadhrani H., Ben Smail R., Driss A., Jouini T. // Acta Cryst. – 2006. – **E62**. – P. m146 – m148.
44. Ben Smail R., Chebbi H., Driss A. // Acta Cryst. – 2007. – **E63**. – P. m1859 – m1860.
45. Chebbi H., Ben Smail R., Zid M.F. // J. Struct. Chem. – 2016. – **57**. – P. 632 – 635.
46. Maciček J., Jordanov A. // J. Appl. Cryst. – 1992. – **25**. – P. 73 – 80.
47. Duisenberg A.J.M. // J. Appl. Cryst. – 1992. – **25**. – P. 92 – 96.
48. Harms K., Wocadlo S. XCAD4, Program for the reduction of CAD4 diffraction data. – University of Marburg, Germany, 1995.
49. Farrugia L.J. // J. Appl. Cryst. – 1999. – **32**. – P. 837 – 838.
50. North A.C.T., Phillips D.C., Mathews F.S. // Acta Cryst. – 1968. – **A24**. – P. 351 – 359.
51. Sheldrick G.M. // Acta Cryst. – 2008. – **A64**. – P. 112 – 122.
52. Brandenburg K. DIAMOND, Version 3.1e, Crystal Impact GbR, Bonn, Germany, 2007.
53. Tarasiewicz J., Gagor A., Jakubas R., Kulicka B., Baran J. // J. Mol. Struct. – 2011. – **1002**. – P. 28 – 36.
54. Owczarek M., Jakubas R., Majerz I., Baran J. // Chem. Phys. – 2012. – **405**. – P. 167 – 174.
55. Ivanova B.B., Arnaudov M.G., Mayer-Figge H. // Polyhedron. – 2005. – **24**. – P. 1624 – 1630.
56. Kowalczyk I., Katrusiak A., Komasa A., Szafran M. // J. Mol. Struct. – 2011. – **994**. – P. 13 – 20.
57. Nakamoto K. Infrared, Raman Spectra of Inorganic, Coordination Compounds, 5th edn. – New York: Wiley-Interscience, 1997.
58. Samanta B., Chakraborty J., Shit S., Batten S.R., Jensen P., Mitra S. // Z. Naturforschung. – 2007. – **62b**. – P. 495 – 500.
59. Sharma R.P., Sharma R., Bala R., Salas J.M., Quiros M. // J. Chem. Crystallogr. – 2005. – **35**. – P. 769 – 775.
60. Karmakar R., Choudhury C.R., Gramlich V., Mitra S. // Inorg. Chim. Acta. – 2004. – **357**. – P. 3785 – 3788.
61. Chen X.Y., Zhao B., Cheng P., Ding B., Liao D.Z., Yan S.P., Jiang Z.H. // Eur. J. Inorg. Chem. – 2004. – P. 562 – 569.
62. Norquist A.J., Heier K.R., Halasyamani P.S., Stern C.L., Poepelmeier K.R. // Inorg. Chem. – 2001. – **40**. – P. 2015 – 2019.
63. Shaikh A.A., Paul D.K., Rahman M.S., Bakshi P.K. // J. Bangladesh Chem. Soc. – 2011. – **24**. – P. 106 – 114.
64. Janiak C. // J. Chem. Soc. Dalton Trans. – 2000. – P. 3885 – 3896.
65. Chao M., Schempp E. // Acta Cryst. – 1977. – **B33**. – P. 1557 – 1564.
66. Anderson F.P., Gallagher J.F., Kenny P.T.M., Lough A.J. // Acta Cryst. – 2005. – **E61**. – P. o1350 – o1353.
67. Halvorson K.E., Patterson C., Willett R.D. // Acta Cryst. – 1990. – **B46**. – P. 508 – 519.
68. Sugiyama J., Meng J., Matsuura T. // Acta Cryst. – 2002. – **C58**. – P. o242 – o246.
69. Savig K.L., Lemmerer A. // Acta Cryst. – 2012. – **E68**. – P. o3361.
70. Fun H.K., Hemamalini M., Rajakannan V. // Acta Cryst. – 2010. – **E66**. – P. o2108.
71. Chérif I., Abdelhak J., Zid M.F., Driss A. // Acta Cryst. – 2011. – **E67**. – P. m1648 – m1649.
72. Sun Q., Liao S., Yao J., Wang J., Fang Q. // Acta Cryst. – 2012. – **E68**. – P. m1160 – m1161.
73. Fun H.K., Jebas S.R., Sinthiya A. // Acta Cryst. – 2008. – **E64**. – P. o697.
74. Ramesh P., Akalya R., Chandramohan A., Ponnuswamy M.N. // Acta Cryst. – 2010. – **E66**. – P. o1000.
75. Clark G.M., Morley R. // Chem. Soc. Rev. – 1976. – **5**. – P. 269 – 295.
76. Kolitsch U. // Z. Kristallogr. – 2003. – **218**. – P. 401 – 402.
77. Jeffrey G.A. In An Introduction to Hydrogen Bonding, Oxford University Press, 1997.